Molecular and Macroscopic Modeling of Phase Separation

Fernando A. Escobedo
School of Chemical Engineering, Cornell University, Ithaca, NY 14853

Recently proposed pseudoensemble Monte Carlo methods are extended in this work to map out diverse phase diagrams (projections of the phase-coexistence hypersurface) of multicomponent mixtures required to characterize fluid-phase equilibrium phenomena and to design separation processes. Within the pseudoensemble framework, the macroscopic models of different equilibrium processes can be readily integrated to the mathematical constraints that specify the thermodynamic state of the system. The proposed Monte Carlo methods allow, for example, the simulation of isopleths and cloud-point lines to compare experimental to simulation data and to test molecular force fields. Applications of this approach include the study of retrograde phenomena in a model natural-gas mixture through simulation of dewlines and coexistence lines at constant vaporization fraction. As demonstrated, pseudoensemble simulations can also be used to generate the thermodynamic data necessary to solve problems encountered in continuous and discontinuous distillation processes.

Introduction

Knowledge of phase equilibria is essential for the design and simulation of multiple separation processes. Several engineering thermodynamic models (TMs), like activity coefficient models and equations of state, are commonly used to generate coexistence data at conditions for which experimental data are not available. Unfortunately, the predictive value of such models is limited, as they often rely on experimental mixture data near the conditions of interest. Molecular modeling has emerged as a complementary tool that can circumvent some of the limitations of TMs. To realize such a potential, however, a critical need exists to develop good molecular force fields and better methods to simulate phase diagrams of complex systems.

Phase diagrams are typically two-dimensional projections of the multidimensional phase-coexistence hypersurface of a system. In a phase diagram, several properties (phase-space coordinates) are constrained to have specific values or to satisfy mathematical relations; those constraints embody experimentally meaningful scenarios. At coexistence, the global free energy of a system is minimized by the formation of two (or more) phases. The problem is to determine when phase separation occurs and to calculate all the properties of such phases from the data that specifies the thermodynamic state. For example, in a single vapor–liquid equilibrium stage, such as that shown in Figure 1, seven common cases can arise (Seader and Henley, 1998), depending on the properties specified to fix the state of the system (the feed stream properties are assumed to be known); these cases include: (1) *isothermal flash*, if T and P are specified (see Figure 1); (2) *nonisothermal flash*, if Q and P are specified; (3) *percent vaporization flash*, if F^I/F and P are specified; (4) *bubble-point temperature*, if $F^I/F = 0$ and P are specified; (5) *bubble-point pressure*, if $F^I/F = 0$ and T are specified; (6) *dew-point temperature*, if $F^{II}/F = 0$ and P are specified; and (7) *dew-point pressure*, if $F^{II}/F = 0$ and T are specified. Similar cases occur in other types of phase equilibrium; for example, *cloud-shadow* points (similar to bubble–dew points) are used for liquid–liquid equilibrium and for polydisperse systems. Furthermore, additional constraints or different specification variables may be relevant to some experimental systems, such as, constraints on chemical potentials, permeability, and surface tension due to reactive, osmotic, and film equilibria, respectively. Methods for direct molecular simulation of all these types of phase equilibria specifications are important because they could allow a more direct comparison between experimental data and simulation results, and even a more direct connection between molecular modeling and practical separation processes.

During the last years, several new Monte Carlo methods have been proposed to study phase-equilibrium specifications

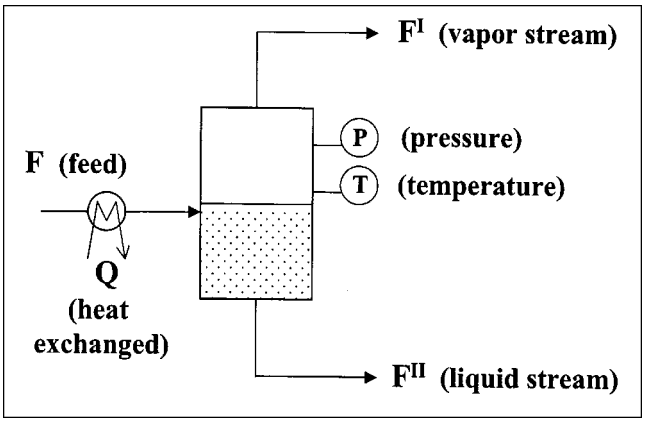

Figure 1. Single stage with one feed stream and two product streams.

Its operation may be continuous or batch.

that are relevant for practical applications. The Gibbs ensemble (GE) technique (Panagiotopoulos, 1987; Panagiotopoulos et al., 1988), the best-known method for direct determination of phase coexistence, simulates ''isothermal'' flash equilibrium, since given the temperature and composition of the overall system, the molecules redistribute between phases so as to satisfy thermodynamic equilibrium and mol balance. The GE requires some prior knowledge of the location of the two-phase region; this can be a disadvantage if such a region is very narrow or difficult to anticipate. Generation of various types of phase diagrams from flash-type-calculation results is not a straightforward task. The mass-balance requirement in the GE method precludes calculations where the incipient phase has negligible volume and the abundant phase has a fixed composition. Finally, transfer moves of complex molecules are more cumbersome in a GE than in other *open* ensembles. Nonisothermal variants of the Gibbs ensemble have been recently reported (Kristof and Liszi, 1998).

The first simulation studies of bubble points for binary and ternary mixtures were conducted by Fischer and coworkers (Vrabec and Fischer, 1995, 1997) by employing variants of the so-called NPT plus test-particle method (NPT + TP). For specified temperature and composition of the liquid phase, these authors employed isothermal–isobaric ensembles to simulate both liquid and vapor phases. An iterative approach is needed, since the pressure, which is a parameter in the ensemble, is not known *a priori*. While an NPT ensemble is a convenient choice to describe the fixed-composition abundant phase (such as the liquid), its use for the vapor phase requires the simulation of several state points if phase-equilibrium conditions are to be found. This problem becomes more severe as the number of components increases. If the initial points lie close enough to the coexistence region, then only one iteration of the method is required to locate the bubble point; an iteration is essentially an extrapolation of thermodynamic properties based on the data collected at the simulated states.

To simulate phase equilibrium for an arbitrary specified situation, we need to know the parameters for the particular statistical mechanical ensemble adopted (such as the temperature and the species chemical potentials in a grand canonical ensemble). Because available ensembles (like the GE) can only simulate very limited cases, a general framework is needed to establish a connection between arbitrary specifications of phase equilibria and the parameters of an arbitrary ensemble; pseudoensembles (PEs) provide such a framework (see Figure 2). PE methods were originally formulated as a way of mimicking the behavior of one ensemble by conducting the simulation in another ensemble (Mehta and Kofke, 1995; Camp and Allen, 1996; Escobedo and dePablo, 1997). It has been shown recently that PE methods can be used to unite seemingly different methods for simulation of fluid-phase equilibrium; the key differences originate in the underlying approximations employed to calculate (through extrapolation) the coexistence properties and in the degree of coupling between the phases (Escobedo, 1998). In particular, NPT + TP methods can be seen as variants of PE techniques, and the GE technique can be closely emulated by special variants of PEs (Camp and Allen, 1996).

PEs can be used to locate a coexistence region if two initial states are known, corresponding to the two distinct phases, and a gradual stepwise extrapolation is performed. If the initial states are already at coexistence, then the extrapolation can be designed to be an integration process to map a coexistence line and the PE becomes a Gibbs-Duhem integration (GDI) scheme (Kofke, 1993). Bubble–dew lines have been simulated by employing open (grand canonical) ensemble simulations (Escobedo, 1998, 1999). Although isothermal–flash calculations have been described in the context of

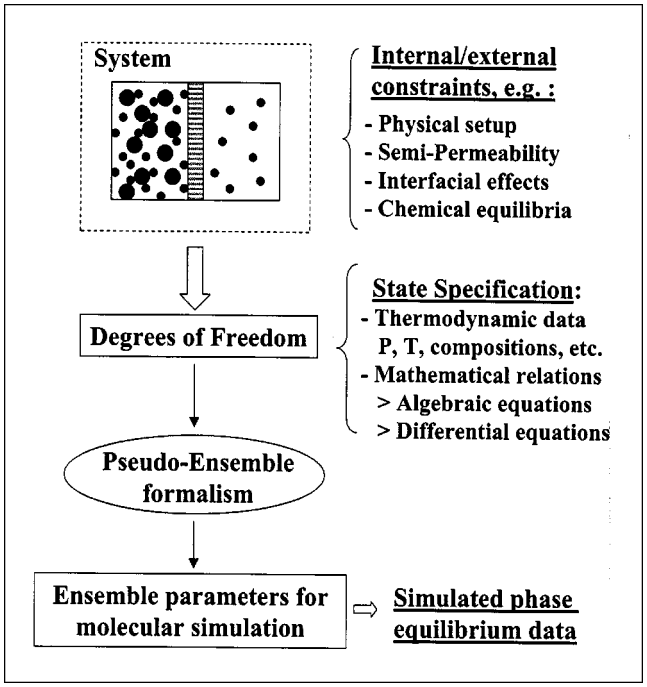

Figure 2. Role of pseudoensembles as a bridge between arbitrary phase equilibrium specifications and the parameters of an arbitrary ensemble.

The internal/macroscopic constraints of a system shape the way phase equilibrium can be specified; the ensemble parameters are needed to perform molecular simulations.

PE methods (Escobedo, 1998, 1999; Spyriouni et al., 1998), those calculations did not account for the mass-balance constraints of true flash operations. Kofke and Henning (1999) have recently shown that bubble–dew lines can also be mapped out by employing GDI with semigrand ensembles; such ensembles are particularly useful when the components in the mixture are relatively similar (in both size and shape), as identity-exchange moves allow efficient configurational sampling (Kofke, 1999). It should also be pointed out that PE methods closely related to the GE technique have also been proposed for ''direct'' simulation of bubble-point pressure calculations (Escobedo, 1999; Ungerer et al., 1999); however, analogous implementations for other single-stage equilibria (like dew points) are more challenging.

The ability to simulate phase equilibrium under arbitrary constraints or specifications can facilitate the identification of peculiar phase phenomena (such as retrograde condensation) and the design of separation processes. Residue-curve maps (which represent the evolution of the liquid composition in a simple Rayleigh batch distillation) and distillation-curve maps (which describe the evolution of liquid composition in a continuous distillation at total reflux) can be effectively used to determine feasible distillation sequences for nonideal mixtures (not only for distillation operations but also for liquid–liquid extraction). Such maps can be simulated by suitable formulations of PEs and GDI. Furthermore, the simulation of a continuous multistage separation column can be aided by molecular simulation data. In all these cases, a molecular simulation approach is particularly attractive when a little-known substance is present or when the systems exhibit phase behavior that is not properly characterized by other means.

In this work, a general formulation is presented to simulate all common cases of single-stage phase equilibrium by using PEs and GDI with open ensembles. It is shown how the proposed methodology can be employed to trace phase diagrams to study different phase equilibria phenomena and system configurations; in particular, to study retrograde condensation phenomena in natural gas, to obtain residue-curve and distillation-curve maps for a ternary mixture, and to conduct distillation column simulations. Mixtures of low-molecular-weight alkanes have been chosen as test beds for this work.

The rest of the article is organized as follows. The methodological framework is presented in the next section, followed by several applications of such a framework to generate phase diagrams and to solve distillation problems. In the last section, a few concluding remarks are summarized.

Simulation of Single-Stage Coexistence with Open Ensembles

Formulation

A PE approach is formulated here to encompass all common types of single-stage equilibrium calculations. Only those theoretical aspects relevant to this work are reviewed here, and readers are referred to the original references for further details on the methods (Escobedo, 1998, 1999). For concreteness, a two-phase equilibrium is assumed (phases I and II). PE simulation of phase equilibrium requires the knowledge of *at least* one initial state lying on the stable thermodynamic region for each phase; such set of states will be referred to as point ''1.'' Point 1 provides the basis for finding the coexistence conditions of the system for a given specification. If point 2 is at coexistence, then the pressure $P(2)$, the temperature $T(2)$, and the chemical potential of each species $\mu_i(2)$ (for $i=1, 2, \ldots, m$, where m is the number of components) must be equal between phases. The ''working'' equations that need to be solved will depend on the input data (associated with state 2). The following equations are relevant to our analysis:

$$\beta(2)P(2) = \langle \beta(2)P(2)\rangle^{I} \tag{1}$$

$$\beta(2)P(2) = \langle \beta(2)P(2)\rangle^{II} \tag{2}$$

$$z_i = \psi x_i(2)^{I} + (1-\psi)x_i(2)^{II} \qquad i=1, 2, \ldots, m-1, \tag{3}$$

where

$$x_i(2)^{I} = \langle x_i(2)\rangle^{I} \tag{4}$$

$$x_i(2)^{II} = \langle x_i(2)\rangle^{II}, \tag{5}$$

and where the symbol $\langle\ \rangle$ denotes ensemble average, for example, the value of the properties evaluated (or extrapolated) from simulation data, $\beta = 1/(k_B T)$ (k_B is Boltzmann constant), z_i is the overall mol fraction of component i in the feed (total moles $= F = F^{I} + F^{II}$), x_i is the mol fraction of

Table 1. Variables, Equations, and Degrees of Freedom for Phase Equilibria Calculations with Open Ensembles (m = number of components)

Variables		Number	Equations		Number
$P(2)$,		1	$P(2) = \langle P(2)\rangle^{I}$,	Eqs. 1, 10	1
$\beta(2)$,	$[=1/k_B T(2)]$	1	$P(2) = \langle P(2)\rangle^{II}$,	Eqs. 2, 10	1
$\nu_i(2)$,	$1 \le m$	m			
z_i,	$1 \le i \le m-1$	$m-1$	$z_i = \psi x_i(2)^{I} + (1-\psi)x_i(2)^{II}$,	Eq. 3	$m-1$
$x_i(2)^{I}$,	$1 \le i \le m-1$	$m-1$	$x_i(2)^{I} = \langle x_i(2)\rangle^{I}$,	Eqs. 4, 11	$m-1$
$x_i(2)^{II}$,	$1 \le i \le m-1$	$m-1$	$x_i(2)^{II} = \langle x_i(2)\rangle^{II}$,	Eqs. 5, 11	$m-1$
ψ,		1	$\psi = [h_F^* - h(2)^{II}]/[h(2)^{I} - h(2)^{II}]$	Eq. 6	1
$h(2)^{I}$,		1	$h(2)^{I} = \langle h(2)\rangle^{I}$,	Eqs. 7, 12, 13	1
$h(2)^{II}$,		1	$h(2)^{II} = \langle h(2)\rangle^{II}$,	Eqs. 8, 12, 13	1
h_F^*,		1			
Total number of variables $4m+3$			Total number of equations		$3m+2$
Total number of degrees of freedom			$=(4m+3)-(3m+2)=m+1$		

component i (in the corresponding phase), and $\psi = F^I/F$ is the fraction of moles (from the feed F) in phase I, which can be expressed in terms of thermal properties:

$$\psi = \left[h_F^* - h(2)^{II} \right] / \left[h(2)^I - h(2)^{II} \right], \tag{6}$$

where $h_F^* = h_F + q$ is the sum of the enthalpy of the feed (h_F) and the amount of heat exchanged per mol of feed (q); h is the molar enthalpy of the corresponding stream, for example,

$$h(2)^I = \langle h(2) \rangle^I = \langle u(2) \rangle^I + P(2)^I \langle v(2) \rangle^I \tag{7}$$

$$h(2)^{II} = \langle h(2) \rangle^{II} = \langle u(2) \rangle^{II} + P(2)^{II} \langle v(2) \rangle^{II}, \tag{8}$$

where u denotes molar energy and v denotes molar volume. For an arbitrary property w, $\langle w(2) \rangle$ is a function of the open ensemble parameters; for convenience, we write this relationship as

$$\langle w(2) \rangle = w\{ \beta(2), \nu_1(2), \nu_2(2), \ldots, \nu_m(2) \}, \tag{9}$$

where $\nu_i = \beta\mu_i$ is an effective, dimensionless chemical potential for species i.

The global structure of the mathematical problem is outlined in Table 1; for the sake of generality, the independent variables chosen are all the intensive parameters of the open ensemble: $\beta(2)$ and all $\nu_i(2)$'s, plus other properties that may be related to the input data: the pressure $P(2)$, mol fractions of the feed and coexisting phases, ψ, and the enthalpies. Note that only "$m-1$" mol fractions are considered per phase, since the condition that their sum is unity is implicit.

As shown in Table 1, $m+1$ independent variables need to be specified to determine state 2. A particular set of input data determines a particular type of phase equilibrium calculation; specific choices are discussed next ($m > 1$):

1. *Percent-Vaporization Pressure Calculation.* In this case, the $m+1$ input data are $\beta(2)$, ψ, and the $m-1$ mol fractions z_i. The working equations for this case are Eqs. 1–5; because the value of ψ is specified, Eqs. 6–8 are unnecessary to solve the problem. *Bubble- and dew-point pressure* calculations are special cases that correspond to $\psi = 0$ and $\psi = 1$, respectively. If ψ were specified on a mass basis, then weight fractions should be used instead of mol fractions in Eqs. 3–5.

2. *Percent-Vaporization Temperature Calculation.* In this case, the $m+1$ input data are $P(2)$, ψ, and the $m-1$ mol fractions z_i. The working equations for this case are again Eqs. 1–5; Eqs. 6–8 are irrelevant for this calculation. *Bubble- and dew-point temperature* calculations correspond to the choice of $\psi = 0$ and $\psi = 1$, respectively.

3. *Isothermal Flash Calculation.* Here, the $m+1$ input data are $\beta(2)$, $P(2)$, and the $m-1$ mol fractions z_i. The working equations for this case are Eqs. 1–5. However, if $m = 2$ the solution only requires Eqs. 1 and 2; the feed composition is only necessary if ψ needs to be calculated, which would then require the use of Eq. 3. In general, ψ can be removed from the analysis by eliminating it from Eq. 3, thereby leaving only $m-2$ independent equations for the z_i.

4. *Nonisothermal Flash Calculation.* In this case, the $m+1$ input data are $P(2)$, h_F^* ($= q + h_F$), and the $m-1$ mol fractions z_i. The working equations for this case are Eqs. 1–8. A special case arises when $q = 0$, for example, the adiabatic or *isoenthalpic* flash calculation. Equation 6 applies to a continuous (open) system; for a closed isometric system, h in such an equation should be replaced by u.

Levels of approximation

To solve Eqs. 1–8, the exact form of Eq. 9 must be specified. Because the input data for any type of phase-equilibrium calculation do not match the open ensemble parameters $\beta(2)$ and the $\nu_i(2)$, the ensemble parameters at coexistence need to be initially "extrapolated" based on previous data of the system; for example, simulation results from point 1 (or from many previous points). Depending on the extrapolation method employed to accomplish this, a connection between pseudoensembles and other methods for phase equilibrium simulation can be established. The connection between histogram reweighting (an infinite-order extrapolation scheme), PE, and GDI formulations (low-order extrapolation schemes) has been described elsewhere (Escobedo, 1998, 1999).

For simplicity, first-order extrapolation formulas are employed in this work. The following equations are relevant to Eqs. 1, 2, 4, 5, 7, and 8:

$$\langle \beta(2) P(2) \rangle^J = \langle \beta(1) P(1) \rangle^J - \frac{\overline{U}^J}{V^J} \Delta\beta^J + \sum_{i=j}^{m} \overline{\rho}_j^J \Delta\nu_j^J \tag{10}$$

$$\langle x_i(2) \rangle^J = \langle x_i(1) \rangle^J - \overline{\sigma}\left(x_i^J, U^J \right) \Delta\beta^J + \sum_{j=1}^{m} \overline{\sigma}\left(x_i^J, N_j^J \right) \Delta\nu_j^J \tag{11}$$

$$\langle u(2) \rangle^J = \langle u(1) \rangle^J - \overline{\sigma}\left(u^J, U^J \right) \Delta\beta^J + \sum_{j=1}^{m} \overline{\sigma}\left(u^J, N_j^J \right) \Delta\nu_j^J \tag{12}$$

$$\langle v(2) \rangle^J = \langle v(1) \rangle^J - \overline{\sigma}\left(v^J, U^J \right) \Delta\beta^J + \sum_{j=1}^{m} \overline{\sigma}\left(v^J, N_j^J \right) \Delta\nu_j^J, \tag{13}$$

where the superscript J can be either I or II to denote the corresponding phase; $\rho_j = N_j/V$ is the molecular density of species j; the symbol Δ denotes the difference between states, for example, $\Delta\beta = \beta(2) - \beta(1)$; $\sigma(w_i, w_j) = \langle w_i w_j \rangle - \langle w_i \rangle \langle w_j \rangle$ is the covariance between w_i and w_j; and the $\sigma(w_i, w_j)$'s are fluctuation quantities that are easily measured during a simulation (see, for example, the appendix of Escobedo, 1998).

In Eqs. 10–13, overlined symbols, to be referred to as "$\overline{w}$-coefficients," identify measurable quantities that, depending on how they are evaluated, lead to two different modes of calculation: an "explicit" mode and an "implicit" mode:

1. In the *explicit* mode, $\bar{w} = \langle w(1) \rangle$ for any property w. Equations 10–13 are then explicit extrapolation formulas.

2. In the *implicit* mode, $\bar{w} = [\langle w(1) \rangle + \langle w(2) \rangle]/2$, for any property w. Equations 10–13 are then implicit extrapolation formulas. A predictor step is required to start the calculation; if both phases are simulated concurrently, convergence to coexistence conditions (at state 2) is achieved by ''on-the-fly'' corrector steps that update the $\bar{w}$-coefficients.

Higher-order predictor and corrector schemes could also be employed; for this purpose, the $\bar{w}$-coefficients must be suitably reformulated in terms of properties measured at more than one previous point (Escobedo, 1999). With the use of Eqs. 10–13, all single-stage phase-equilibrium calculations are reduced to a set of algebraic equations that can be readily solved by numerical methods.

If point 1 is a coexistence point already, then repeated PE simulations can be used to trace coexisting lines; such a scheme effectively becomes a GDI method (Kofke, 1993). When mapping a coexistence line, explicit PE simulations need only be run near the phase boundary; coexistence conditions can then be estimated by extrapolation. When consecutive points are simulated, the pressure need only be measured at the first point (such as by using the virial formula), since $P(2)$ is either specified or is calculated from Eq. 10. In practice, the pressure should be measured at select points to prevent systematic deviations.

Applications

Simulations were conducted for a total of $3-5 \times 10^4$ Monte Carlo cycles per state point (or integration step) (Allen and Tildesley, 1987). Thermal equilibration was accomplished through a combination of translation, rotation, reptation, flip, and configurational-bias moves (de Pablo et al., 1992; Frenkel and Smit, 1996). Configurational-bias and expanded ensemble moves (Escobedo and de Pablo, 1996) were used to facilitate the insertion-deletion of molecules. A cutoff radius of 11 Å was employed for Lennard-Jones interactions and standard tail corrections were implemented; for unlike pair interactions, the standard Lorentz-Berthelot combining rules were employed (Allen and Tildesley, 1987). System sizes varied from 400 to 4,000 interaction sites in a simulation box; the larger sizes correspond to systems with more components and higher densities. Unless stated otherwise, the force field for ethane is from Spyriouni et al. (1998) and that for longer alkanes is from Nath et al. (1998).

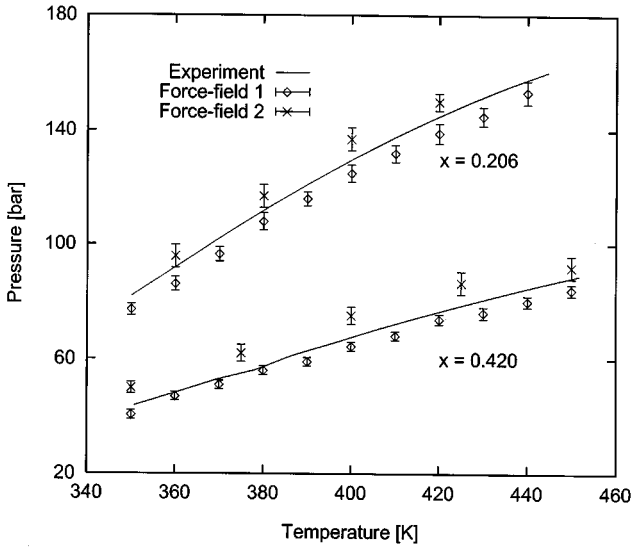

Figure 3. Isopleths for eicosane–ethane system.

x denotes the mol fraction of eicosane in the liquid. Experimental data from Peters et al. (1987), and simulation data from PE runs for the Nath et al. (1998)/Spyriouni et al. (1998) potential model (force field 1, diamonds), and for the Errington and Panagiotopoulos (1999) model (force field 2, crosses).

Isopleths

Figure 3 shows bubble-point curves for a mixture of ethane-eicosane using the Spyriouni/Nath potential model; for each curve, multistep explicit PE simulations were conducted from the lowest to the highest temperature. Results are also included for the force field recently proposed by Errington and Panagiotopoulos (1999). The deviations between experimental and simulation data observed in Figure 3 reflect some of the limitations of the force fields employed; while one of the potential models tends to consistently underestimate the bubble-point pressure, the other tends to overestimate it. Even if the combined uncertainities of experimental (Peters et al., 1987) and simulation data are taken into account, the agreement between simulation and experiment is only fair. This limitation illustrates one of the great needs of molecular simulation methodology: good potential energy models; indeed, several alternative, more detailed models have been recently proposed for alkanes (such as Chen

Table 2. Composition of Natural-Gas Mixture and Simulated Composition of Phases at 310.93 K and 103.4 bar*

Component	Feed Compositions	Gibbs Ensemble		Open Pseudoensemble	
		Vapor	Liquid	Vapor	Liquid
Methane	0.824	0.895(4)	0.407(13)	0.895(4)	0.392(14)
Ethane	0.043	0.0413(6)	0.053(3)	0.0410(5)	0.053(2)
Propane	0.035	0.0274(5)	0.080(3)	0.0283(8)	0.082(3)
Butane	0.046	0.0265(5)	0.158(6)	0.0262(6)	0.153(5)
Pentane	0.013	0.0052(3)	0.058(4)	0.0054(3)	0.060(4)
Hexane	0.010	0.0024(3)	0.053(4)	0.0026(2)	0.055(3)
Nonane	0.029	0.0016(2)	0.190(15)	0.0016(1)	0.205(15)
ρ (g/cm^3)		0.0961(8)	0.535(10)	0.0963(7)	0.543(10)
ψ		0.854		0.852	

*Compositions in molar fraction.

et al., 1998; Ungerer et al., 2000). Because bubble-point and cloud-point curves are often reported experimentally, PEs can facilitate testing and development of molecular force fields.

Retrograde phenomena

Natural gas is a complex mixture of predominantly light hydrocarbons whose majority component is typically methane. Variations of pressure in the reservoir can lead to a phenomenon known as retrograde condensation (Ahmed, 1989). Because the phase behavior of a ''retrograde'' gas or of a condensate gas is quite sensitive to the composition of the gas (in particular, to the content of ''heavies''), molecular simulation can provide a more accurate description of retrograde phenomena for such systems. Neubauer et al. (1999) have recently presented a molecular simulation study of the volumetric properties of natural gas; most of their results were generated by NPT ensemble runs while a few GE simulations were performed to locate the region of retrograde condensation.

To illustrate how PE methods can be used to study retrograde phenomena, we adopted the variant of system I that Neubauer et al. used for their GE simulations; such a system is a simplified representation of a reported natural-gas mixture. The composition of this model natural-gas mixture is shown in Table 2 along with our results from GE simulations and from ''Isothermal-Flash'' PE simulations (as described in the second section) at $T = 310.93$ K and $P = 103.4$ bar. As shown in Table 2, results from the two methods agree within the error bars of the simulations. A GE provides a more straightforward route to a flash calculation; for the system at hand, however, some preliminary calculations were necessary to ensure that the sizes of both phases were sufficiently large to accommodate at least a few molecules of the most dilute component. This resulted in a system with nearly 3000 molecules. This type of problem is much less severe for PE simulations, since the overall composition of the system (both phases) need not be that of the feed; however, at least an iteration of the calculation is needed to predict the coexistence properties (unless the reference point is already near the desired state). The starting point for the PE series in this case was a dew point obtained for $P = 103.4$ bar (temperature $T = 415.6$ K); the isothermal-flash point at $T = 310.93$ K was located with two iterations.

For the conditions indicated in Table 2, $\psi \sim 0.85$, proper system sizing for a Gibbs ensemble approach becomes more troublesome as $\psi \to 1$ (or as $\psi \to 0$). The retrograde phenomenon is conveniently analyzed by mapping $P - T$ curves at constant ψ and in particular for the natural-gas dewline ($\psi = 1$). Figure 4 shows such calculations for the natural-gas mixture of Table 2. The full and dashed lines are predictions of the Soave (1972) and the Peng-Robinson (1976) equations of state, respectively (all binary interaction parameters are set to zero). Simulation and theory both predict retrograde phenomena, that is, partial liquefaction of a gas as it is decompressed and enters the region enclosed by the dewline; the relative degree of liquefaction can be visualized by the simulated lines for fixed vaporized fraction ($\psi = 0.95$ and $\psi = 0.9$). The dewline was started by simulating the $P = 103.4$-bar dew-point temperature; the rest of the curve was obtained by explicit PE steps for both increasing and decreasing pressures. Fixed-ψ data points were obtained by explicit PE steps starting from the corresponding dew points (at the same pressure).

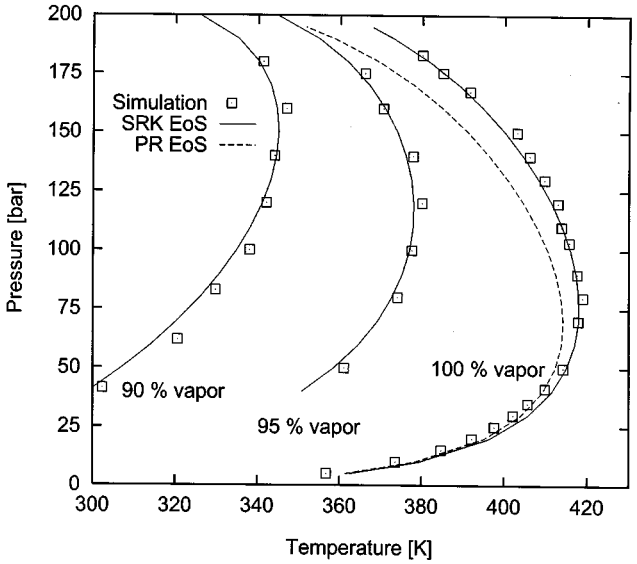

Figure 4. Constant percent of vaporization curves for the 7-component ''natural gas'' mixture of Table 2.

——, predictions of the Soave-Redlich-Kwong equation of state; – – – –, the Peng-Robinston equation of state. Simulation data (□) were obtained through *explicit* PE calculations (for specified pressure) with the force field of Nath et al. (1998)/Spyriouni et al. (1998); error bars are about two times the size of the symbols.

Since no experimental dewline exists for this system, it is not possible to test the quality of the force field employed in these simulations. Simulation results agree well with those obtained from the Soave-Redlich-Kwong (SRK) equation of state (lines in Figure 4); they deviate significantly, however, from the predictions of the Peng-Robinson equation of state at high pressures. Both cubic equations of state predict that the dewline critical point is located slightly above 200 bar and $T < 350$ K; PE simulations become unstable near the mixture critical point and no attempt was made to approach it or to estimate it by finite-size scaling.

Residue-curve and distillation-curve maps

Residue-curve maps show the evolution of the heavy phase (that is, the one left in the still) in a Rayleigh batch distillation. Since the light phase (vapor) is continuously removed from the system at constant pressure, the compositions of the heavy (II) and light (I) phases are related to the number of moles N in the heavy phase through the mol balance: $d(Nx_i^{II}) = x_i^I dN$, which leads to the following equation:

$$\frac{dx_i^{II}}{d\zeta} = x_i^{II} - x_i^I, \qquad i = 1, 2, \ldots, m-1, \tag{14}$$

where $\zeta = -\ln(N)$ is a dimensionless parameter that increases monotonically as the distillation advances. The integration of Eq. 14 essentially entails the calculation of successive bubble-temperature points for a liquid whose composition changes from step to step in a prescribed manner. Kofke and Henning (1999) have described a suitable simulation scheme in the context of a semigrand ensemble GDI method. Consider, for example, a simple rectangle rule of integration for Eq. 14:

$$x_i(2)^{II} = x_i(1)^{II} + \Delta\zeta\left[x_i(1)^{II} - x_i(1)^{I}\right], \qquad i = 1, 2, \ldots, m-1 \quad (15)$$

where the integration stepsize, $\Delta\zeta$, is a preset quantity. A residue-curve calculation can then be cast into a variant of single-stage phase equilibrium by employing the same formalism described in the second section; one integration step of Eq. 14 corresponds to a PE bubble-temperature calculation, wherein the "feed" composition data, $z_i = x_i^{II}(2)$, evolves according to Eq. 15 (this can be seen as an example of generalized bubble-dew curves; Escobedo, 1999).

Distillation-curve maps depict the changes in the composition of a heavy phase as it passes through different ideal stages in a continuous distillation column that is operated at total reflux. Under these conditions, the composition of a liquid exiting a stage (phase *II*) is identical to that of the incoming vapor (phase *I*). Let the current stage correspond to state 1; then if the stage immediately *above* is identified as state 2:

$$x_i(2)^{II} = x_i(1)^{I}, \qquad i = 1, 2, \ldots, m-1. \quad (16)$$

Conversely, if now the stage immediately *below* is identified as state 2, then

$$x_i(2)^{I} = x_i(1)^{II}, \qquad i = 1, 2, \ldots, m-1. \quad (17)$$

Thus, stage-up calculations entail bubble-temperature simulations, where the liquid composition is set equal to that of vapor coming from the stage underneath (Eq. 16), while stage-down calculations entail dew-temperature simulations, where the vapor composition is set equal to that of the liquid coming from the stage above (Eq. 17).

Both distillation curves and residue curves are usually employed to analyze nonideal ternary systems (Doherty and Perkins, 1978); for illustration purposes, however, we consider a fairly ideal system composed of propane, butane, and pentane. The results are shown in Figure 5. In this example, Eq. 17 and explicit PE simulations were used to step down the distillation column. A trapezoid rule was employed instead of Eq. 15. As expected (Seader and Henley, 1998), the shape of the residue curve and distillation curve maps are similar and would convey similar information in terms of identifying feasible sequences for nonideal systems.

Multistage distillation columns

The equilibrium-based mathematical modeling of multiple-section, countercurrent cascades entails the use of

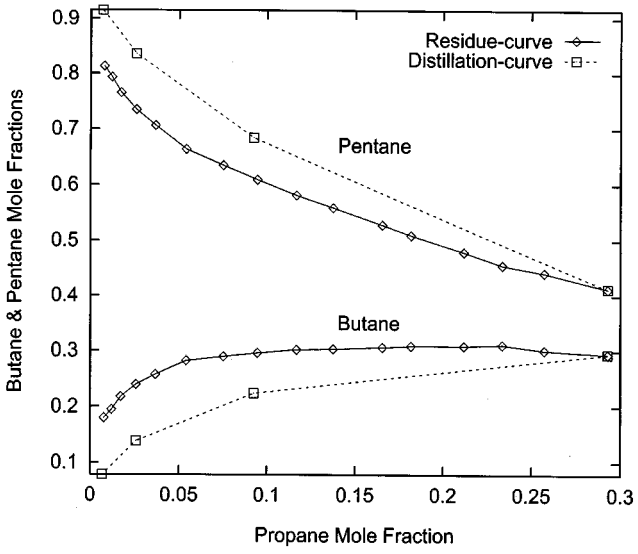

Figure 5. Simulated residue curve (—◇—) and distallation curve (––□––) for a mixture of propane, butane and pentane at a constant pressure of 6.895 bar.

Force field from Nath et al. (1998). The initial state is depicted by the rightmost points (bubble temperature = 329 K). The liquid-phase compositions evolve from right to left. Error bars commensurate to the size of the symbols.

component balances, energy balances, and phase equilibria relations; these are often called the MESH equations. For each (generalized) stage "j" in the column, we have

$$F_j z_{i,j} + \sum_{J=I}^{II}\left[F_{j+k}^{J} x_{i,j+k}^{J} - \left(F_j^J + G_j^J\right) x_{i,j}^{J}\right] = 0$$

$$x_{i,j}^{I} - K_{i,j} x_{i,j}^{II} = 0$$

$$\sum_{i=1}^{m} x_{i,j}^{I} - 1 = \sum_{i=1}^{m} x_{i,j}^{II} - 1 = 0$$

$$F_j h_{F_j} - q_j + \sum_{J=I}^{II}\left[F_{j+k}^{J} h_{j+k}^{J} - \left(F_j^J + G_j^J\right) h_j^J\right] = 0, \quad (18)$$

where G denotes a side stream, $k = 3 - 2J$, and the K's are the "K-values," that is, the ratios of vapor to liquid mol fraction of each component; the meaning of the other symbols is consistent with our discussion related to Figure 1 and Eqs. 3–8. Efficient methods exist to solve such a set of coupled equations (Seader and Henley, 1998). Such models rely on semiempirical "thermoydnamic models" TMs (like equations of state) to provide the thermodynamic properties of the system. Molecular modeling could improve the predictive capability of the approach if, lacking experimental data, simulation data are used to *parameterize* a TM. However, the selection and parameterization of a TM can be accomplished in a number of ways; alternative approaches should be investigated to identify promising strategies. In this section, an approach is described wherein *piecewise* parameterization of a

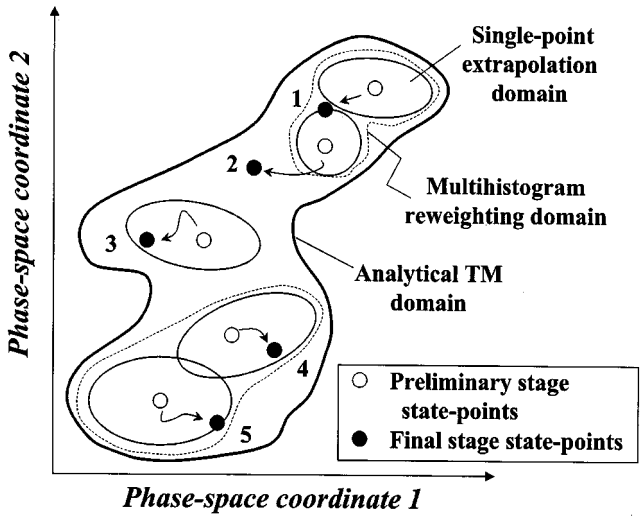

Figure 6. Mapping of thermodynamic phase space for multistage phase-equilibria.

For simplicity, a 2-D phase space and five stages are assumed. ●, final (equilibrium) states for the stages; ○, simulated first guesses of those states. Three distinct extrapolation domains are: (1) single-point domains around each simulated point (ellipses); (2) multi-HR domains that can combine simulated data from different points (dashed contours); and (3) TM domains (thick closed contour). The piecewise parameterization of the TM is assumed to allow a more comprehensive mapping of phase space than the multi-HR approach. In general, additional points may need to be simulated to enclose all relevant regions.

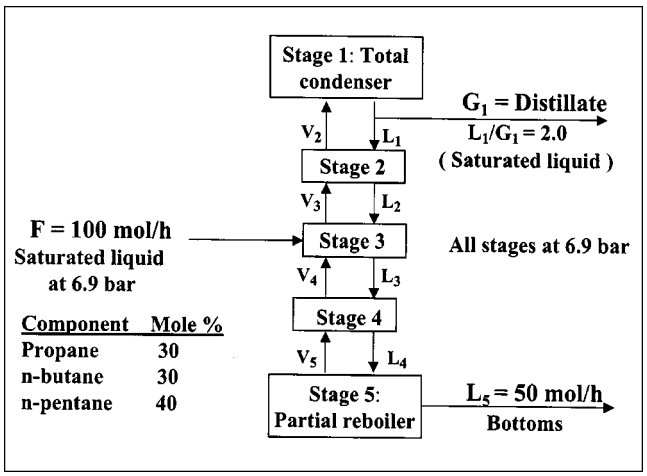

Figure 7. Specifications of a test distillation column.

TM is performed; that is, by using different TM parameters for different subregions of phase space. To do that, simulation data must be generated to probe the portion of phase space that is relevant to the process. Such a task can be accomplished by a histogram reweighting method (Ferrenberg and Swendsen, 1987, 1988; Potoff and Panagiotopoulos, 1998) or a lower-order scheme coupled to a PE formulation to handle the phase-equilibria specifications. The role of the TM is twofold: (1) to provide local correlations to facilitate iterative calculations, and (2) to extend the extrapolative capabilities associated with the simulation data. The concept is illustrated in Figure 6. These ideas will be implemented for the ''design'' problem wherein the number of stages, pressure, condition and location of all feeds, and flow rates and locations of product streams are all specified. Figure 7 shows a sample column specification (Seader and Henley, 1998). Borrowing from concepts of inside-out methods (Boston and Sullivan, 1974), the following three-step process is suggested.

Step 1. If an approximate analytical TM is available for the system, use it to solve the MESH model and obtain estimates of the temperatures, flow rates, compositions, and enthalpies at each stage of the column. If no such TM is available, simulate a few points of a *distillation-curve map* for the composite feed (the first two points would be the feed bubble and dew points); use these data to parameterize an analytical TM model.

Step 2. Conduct bubble-point simulations at select stages and for the liquid compositions found from Step 1. Collect histograms (or the moments of the ensemble probability distribution) at each simulated point (including those from Step 1, if any).

Step 3. Use a multihistogram reweighting or a related scheme with the data collected in Step 2 to reparameterize (piecewise) the TM and solve the MESH equations again.

For systems with nonideal behavior, or if conditions vary significantly between stages, the simulations of Step 2 could be performed at every stage and even a global iteration of Steps 2–3 may be required. For concreteness, bubble-point (temperature) simulations are suggested for Step 2; other types of ''single-stage'' calculations could also be performed. If the collected histograms are sharply peaked (such as for large systems), the reweighting scheme of Step 2 effectively reduces to a PE approach, in which case, extrapolation of conditions near a simulated (coexistence) point can be effectively accomplished with the formalism presented in the second section. This low-order reweighting scheme with explicit-mode open PEs will be employed for the ensuing discussion.

For the system of Figure 7, Step 1 was carried out by simulating first the bubble point and the dew point of the feed; simulated K-values and phase enthalpies were fitted to the simple forms:

$$K_i = A_i \exp(-B_i/T) \qquad (i = 1, 2, \ldots, m) \qquad (19)$$

$$h^J = C^J + D^J T \qquad (J = \text{I or II}), \qquad (20)$$

where A, B, C, and D are adjustable parameters. Better models would be needed for less ideal systems. The MESH equations were then solved by employing an in-house program based on the *Theta* method (Holland, 1963), but more advanced methods will be needed for more complex cases. The resulting liquid compositions were used for Step 2 to conduct bubble-point temperature PE simulations at each stage; fluctuation quantities (related to second moments of the ensemble probability density distribution) were collected to allow the use of Eqs. 10–13. For Step 3, the thermodynamic properties at each stage (as required by the distillation program) were not obtained from the TM but from PE extrapolations of the simulation data collected at the corresponding stage. The reason is that Eqs. 19 and 20 are not good TMs (even with stage-specific parameters) and the final

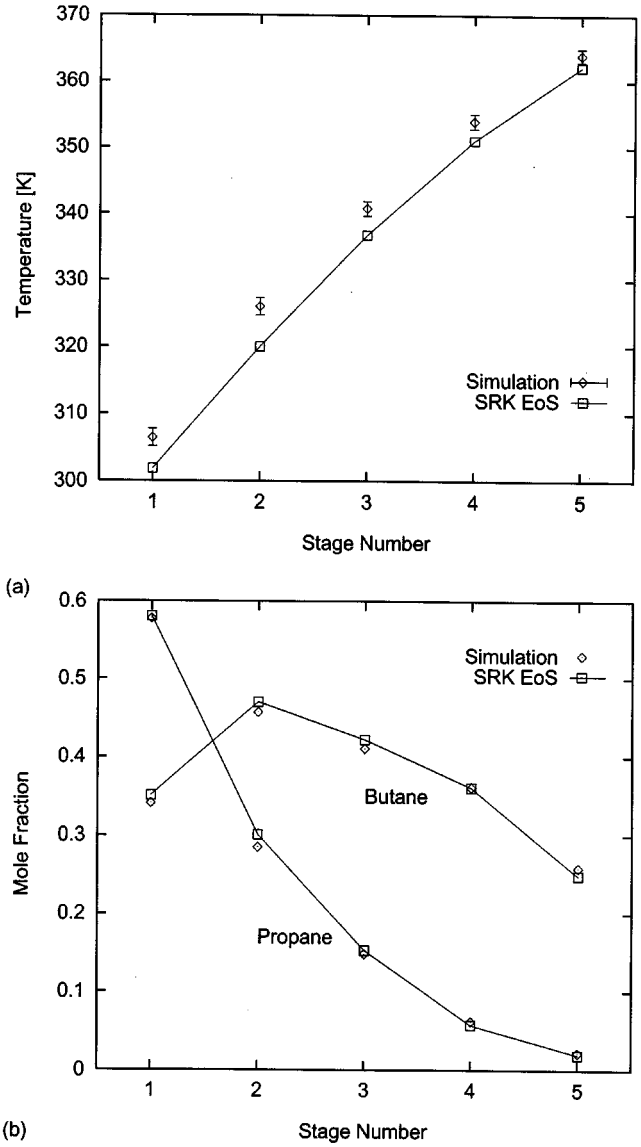

Figure 8. Steady-state temperatures (a) and liquid compositions (b) for the column in Figure 7.

Simulation results are shown by diamonds, predictions from the Soave-Redlich-Kwong equation of state are shown by squares (the lines are drawn to guide the eye). In (b), simulation error bars (omitted for clarity) are commensurate to the size of the squares.

stage states turned out to be within the simulated single-point extrapolation domains. Figure 8 shows the temperatures and liquid compositions from Step 3. Simulation data are seen to agree reasonably well with those obtained when the conventional SRK equation of state is used as the global TM; stage compositions appear to agree better than temperatures.

Conducting simulations at each stage has the advantage that a PE (or GDI) scheme can be used to step from one stage to the next without requiring iterations (only stage 1 required iteration); note also that it is not critical to target accurately the specified liquid compositions (or pressure) in Step 2, since those are simply reference values that need only be ''near'' the final conditions. For columns with numerous stages where compositions do not change much between stages, simulations can be restricted to select stages.

Errors in the results of the proposed scheme arise from the inherent statistical uncertainty of the results at the simulated state points, and from the approximations introduced by the extrapolation scheme adopted (such as truncation errors and method for data analysis). Preliminary calculations indicate that the final results are more affected by the statistical errors (on averages and fluctuation quantities needed for the extrapolations) than by the extrapolation scheme employed. More accurate results can be obtained by running longer runs and (1) by employing a higher-order scheme (such as histogram weighting), provided that statistical errors are small, or (2) by global iteration of Steps 2 and 3, and (3) by using a better TM. Approach (1) requires much longer simulations than approach (2), but the latter requires more numerous runs. For the system studied here, approach (2) was tested and shown to cause inconsequential changes to the final results (such as stage temperatures changed by less than 0.7 K). Further investigation is needed to assess the advantages of higher-order extrapolation schemes and, more importantly, of better TMs. It is important to point out that, in spite of the statistical noise, a simulation-based TM could still be useful for the generation of sensible predictions on the phase behavior of systems containing little-known materials; after all, the uncertainties associated with the quality of the force field adopted (or of any TM for that matter), and with the mapping of ideal stages into real ones, are also significant.

Concluding Remarks

A PE approach has been described for the simulation of typical single-stage phase equilibria, including all seven cases alluded to in the introduction. It has been shown how these single-stage calculations can be applied to map out different types of phase diagrams of practical interest, such as isopleths, residue-curve, and distillation-curve maps, and to generate coexistence data to study retrograde phenomena and to simulate distillation processes.

Other phase-equilibrium calculations can be implemented by employing a similar analysis; for example, the simulation of azeotropes. An azeotrope exists when

$$x_i(2)^I = x_i^{II}(2) \rightarrow \langle x_i(2)^I \rangle = \langle x_i^{II}(2) \rangle, \qquad i = 1, 2, \ldots, m-1. \quad (21)$$

Just as Eqs. 15–17, Eq. 21 can be interpreted as a particular way of specifying the feed-composition degrees of freedom, $z_i = x_i^I = x_i^{II}$. Consequently, finding an azeotrope or mapping an azeotrope line can be accomplished by solving Eqs. 1, 2, and 21; Eqs. 10 and 11 are relevant first-order extrapolation formulas. Pandit and Kofke (1999) have implemented a GDI scheme with semigrand ensembles to trace a locus of azeotropes.

PE and GDI simulations can be formulated and performed in different ensembles; the choice of ensemble type is dictated by the characteristics of the system under investigation. For our work, open ensembles were implemented because an expanded-ensemble formalism is readily implemented to facilitate the insertion–removal of long articulated molecules

(Escobedo and de Pablo, 1996). Open ensembles also lead to simple formulas for the fluctuation quantities needed in Taylor series expansions, like Eqs. 10–13. Other ensembles are to be preferred in certain situations, for example, a semigrand ensemble is indicated if the size asymmetry among components is moderate.

Just as PE and GDI methods can be formulated by using different ensembles, several variants of GE can be formulated by using different base ensembles (Kristof and Liszi, 1998). All single-stage calculations described here could in principle be performed by PE methods closer in spirit to a GE than to a NPT+TP method. In general, flash-type calculations are best suited to a Gibbs ensemble approach, where mass-balance constraints are automatically satisfied. Percent-vaporization calculations, and bubble–dew-point calculations in particular, seem to be better suited to a PE approach.

The common theme of this work has been the combination of molecular and macroscopic modeling to generate phase diagrams suitable for phase-separation studies. The molecular component comes from the force field adopted, and the macroscopic component comes from the set of constraints that the system must satisfy at the macroscopic level. In this context, the specifications for different single-stage calculations, the constraints embodied by Eqs. 14, 16, 17, and the MESH equations (Eqs. 18), are all examples of macroscopic-level models. Simulated residue-curve and distillation-curve maps provide information that can be used to design distillation operations. Also, molecular simulation data could be used in lieu of experimental data to help parameterize a suitable engineering TM for multistage distillation calculations. A variant of such a strategy is to employ a *hybrid* method wherein an engineering TM and a molecular simulation-based TM are concurrently employed to map out the thermodynamic phase space relevant to the process. While the molecular simulation-based TM can be used as the primary TM of the system (as shown in this work), it may not be the optimal approach for complex systems. Further investigation is under way to develop robust strategies that harness the predictive power of molecular simulation and the efficiency of engineering TM to study separation processes; such strategies may prove to be advantageous not only for macroscopic equilibrium-based models but also for rate-based models (Krishnamurthy and Taylor, 1985).

Acknowledgment

The author is grateful to The Camille and Henry Dreyfus Foundation for a new faculty award. He is also grateful to Intel Corporation for the donation to three Pentium-MMX workstations. The author also thanks Prof. Ross Taylor (Clarkson University) for helpful discussions.

Literature Cited

Ahmed, T., *Hydrocarbon Phase Behavior*, Gulf Pub., Houston (1989).
Allen, M. P., and D. J. Tildesley, *Computer Simulation of Liquids*, Clarendon Press, Oxford (1987).
Boston, J. F., and S. L. Sullivan, "A New Class of Solution Methods for Multicomponent, Multistage Separation Processes," *Can. J. Chem. Eng.*, **52**, 52 (1974).
Camp, P. J., and M. P. Allen, "Phase Coexistence in a Pseudo Gibbs Ensemble," *Mol. Phys.*, **88**, 1459 (1996).
Chen, B., M. G. Martin, and J. I. Siepmann, "Thermodynamic Properties of the Williams, OPLS-AA, and MMFF94 All-Atom Force Fields for Normal Alkanes," *J. Phys. Chem. B*, **102**, 2578 (1998).
De Pablo, J. J., M. Laso, and U. W. Suter, "Simulation of Polyethylene Above and Below the Melting Point," *J. Chem. Phys.*, **96**, 2395 (1992).
Doherty, M. F., and J. D. Perkins, "On the Dynamics of Distillation Processes: I," *Chem. Eng. Sci.*, **33**, 281 (1978).
Errington, J., and A. Z. Panagiotopoulos, "A New Potential Model for the n-Alkane Homologous Series," *J. Phys. Chem. B*, **103**, 6314 (1999).
Escobedo, F. A., and J. J. de Pablo, "Expanded Grand Canonical and Gibbs Ensemble Monte Carlo Simulation of Polymers," *J. Chem. Phys.*, **105**, 4391 (1996).
Escobedo, F. A., and J. J. de Pablo, "Pseudo Ensemble Simulations and Gibbs-Duhem Integrations for Polymers," *J. Chem. Phys.*, **106**, 2911 (1997).
Escobedo, F. A., "Novel Pseudo-Ensembles for Simulation of Multicomponent Phase Equilibria," *J. Chem. Phys.*, **108**, 8761 (1998).
Escobedo, F. A., "Tracing Coexistence Lines in Multicomponent Fluid Mixtures by Molecular Simulation," *J. Chem. Phys.*, **110**, 11999 (1999).
Ferrenberg, A. M., and R. H. Swendsen, "New Monte Carlo Technique for Studying Phase Transitions," *Phys. Rev. Lett.*, **61**, 2635 (1988).
Ferrenberg, A. M., and R. H. Swendsen, "Optimized Monte Carlo Data Analysis," *Phys. Rev. Lett.*, **63**, 1195 (1989).
Frenkel, D., and B. Smit, *Understanding Molecular Simulation*, Academic Press, San Diego (1996).
Holland, C. D., *Multicomponent Distillation*, Prentice Hall, Englewood Cliffs, NJ (1963).
Kofke, D. A., "Direct Evaluation of Phase Coexistence by Molecular Simulation via Integration Along the Saturation Line," *J. Chem. Phys.*, **98**, 4149 (1993).
Kofke, D. A., "Semigrand Canonical Monte Carlo Simulation; Integration Along Coexistence Lines," *Adv. Chem. Phys.*, **105**, 405 (1999).
Kofke, D. A., and J. A. Henning, "Thermodynamic Integration Along Coexistence Lines," *Theor. Comput. Chem.*, **7**, 99 (1999).
Krishnamurthy, R., and R. Taylor, "Nonequilibrium Stage Model of Multicomponent Separation Processes," *AIChE J.*, **31**, 449 (1985).
Kristof, T., and J. Liszi, "Alternative Gibbs Ensemble Monte Carlo Implementations: Application in Mixtures," *Mol. Phys.*, **94**, 519 (1998).
Mehta, M., and D. A. Kofke, "Molecular Simulation in a Pseudo Grand-Canonical Ensemble," *Mol. Phys.*, **86**, 139 (1995).
Nath, S. K., F. A. Escobedo, and J. J. de Pablo, "On the Simulation of Vapor-Liquid Equilibria for Alkanes," *J. Chem. Phys.*, **108**, 9905 (1998).
Neubauer, B., B. Tavitian, A. Boutin, and P. Ungerer, "Molecular Simulations on Volumetric Properties of Natural Gas," *Fluid Phase Equilibria*, **161**, 45 (1999).
Panagiotopoulos, A. Z., "Direct Determination of Phase Coexistence Properties of Fluids by Monte Carlo Simulation in a New Ensemble," *Mol. Phys.*, **61**, 813 (1987).
Panagiotopoulos, A. Z., N. Quirke, M. Stapleton, and D. J. Tildesley, "Phase Equilibria by Simulation in the Gibbs Ensemble," *Mol. Phys.*, **63**, 527 (1988).
Pandit, S. P., and D. A. Kofke, "Evaluation of a Locus of Azeotropes by Molecular Simulation," *AIChE J.*, **45**, 2237 (1999).
Peng, D. Y., and D. B. Robinson, "A New Two-Constant Equation of State," *Ind. Eng. Chem. Fundam.*, **15**, 59 (1976).
Peters, C. J., J. L. de Roo, and R. N. Lichtenthaler, "Measurements and Calculations of Phase Equilibria of Binary Mixtures of Ethane + Eicosane: Vapour + Liquid Equilibria," *Fluid Phase Equilibrium*, **34**, 287 (1987).
Potoff, J. J., and A. Z. Panagiotopoulos, "Critical Point and Phase Behavior of the Pure Fluid and a Lennard-Jones Mixture," *J. Chem. Phys.*, **109**, 10914 (1998).
Seader, J. D., and J. H. Henley, *Separation Process Principles*, Wiley, New York (1998).
Soave, G., "Equilibrium Constants from a Modified Redlich-Kwong

Equation of State,'' *Chem. Eng. Sci.*, **27**, 1197 (1972).
Spyriouni, T., I. G. Economou, and D. N. Theodorou, ''Phase Equilibria of Mixtures Containing Chain Molecules Predicted Through a Novel Simulation Scheme,'' *Phys. Rev. Lett.*, **80**, 4466 (1998).
Ungerer, P., A. Boutin, and A. H. Fuchs, ''Direct Calculation of Bubble Points by Monte Carlo Simulation,'' *Mol. Phys.*, **97**, 523 (1999).
Ungerer, P., C. Beauvais, J. Delhommelle, A. Boutin, B. Rousseau, and A. H. Fuchs, ''Optimization of the Anisotropic United Atoms Intermolecular Potential for n-Alkanes,'' *J. Chem. Phys.*, **112**, 5499 (2000).
Vrabec, J., and J. Fischer, ''Vapour Liquid Equilibria of Mixtures from the NpT Plus Test Particle Method,'' *Mol. Phys.*, **85**, 781 (1995).
Vrabec, J., and J. Fischer, ''Vapor-Liquid Equilibria of the Ternary Mixture $CH_4 + C_2H_6 + CO_2$ from Molecular Simulation,'' *AIChE J.*, **43**, 212 (1997).

Manuscript received Oct, 22, 1999, and revision received May 3, 2000.